# Upregulated *ATM* Gene Expression and Activated DNA Crosslink–Induced Damage Response Checkpoint in Fanconi Anemia: Implications for Carcinogenesis

*Kazuhiko Yamamoto,[1,2] Abdallah Nihrane,[1,2] Jason Aglipay,[3] Juan Sironi,[3] Steven Arkin,[1,2] Jeffrey M Lipton,[1,2] Toru Ouchi,[3,4] and Johnson M Liu[1,2]*

[1]The Feinstein Institute for Medical Research, Manhasset, New York, USA; [2]Schneider Children's Hospital, New Hyde Park, New York, USA; [3]Department of Oncological Sciences, Mount Sinai School of Medicine, New York, New York, USA; [4]Systems Genome Biology Program, ENHRI, Feinberg School of Medicine, Northwestern University, Evanston, Illinois, USA

Fanconi anemia (FA) predisposes to hematopoietic failure, birth defects, leukemia, and squamous cell carcinoma of the head and neck (HNSCC) and cervix. The FA/BRCA pathway includes 8 members of a core complex and 5 downstream gene products closely linked with BRCA1 or BRCA2. Precancerous lesions are believed to trigger the DNA damage response (DDR), and we focused on the DDR in FA and its putative role as a checkpoint barrier to cancer. In primary fibroblasts with mutations in the core complex FANCA protein, we discovered that basal expression and phosphorylation of ATM (ataxia telangiectasia mutated) and p53 induced by irradiation (IR) or mitomycin C (MMC) were upregulated. This heightened response appeared to be due to increased basal levels of ATM in cultured *FANCA*-mutant cells, highlighting the new observation that ATM can be regulated at the transcriptional level in addition to its well-established activation by autophosphorylation. Functional analysis of this response using γ-H2AX foci as markers of DNA double-stranded breaks (DSBs) demonstrated abnormal persistence of only MMC- and not IR-induced foci. Thus, we describe a processing defect that leads to general DDR upregulation but specific persistence of DNA crosslinker-induced damage response foci. Underscoring the significance of these findings, we found resistance to DNA crosslinker-induced cell cycle arrest and apoptosis in a *TP53*-mutant, patient-derived HNSCC cell line, whereas a lymphoblastoid cell line derived from this same individual was not mutated at *TP53* and retained DNA crosslinker sensitivity. Our results suggest that cancer in FA may arise from selection for cells that escape from a chronically activated DDR checkpoint.

**Online address: http://www.molmed.org**
**doi: 10.2119/2007-00122.Yamamoto**

## INTRODUCTION

Fanconi anemia (FA) is a genetic disorder that predisposes to bone marrow failure, birth defects, and cancer (1,2). FA is characterized by chromosomal and cellular hypersensitivity to DNA cross-linking agents such as mitomycin C (MMC) and diepoxybutane (DEB). Thirteen FA genes have been identified: *FANCA*, *FANCB*, *FANCC*, *FANCD1/BRCA2*, *FANCD2*, *FANCE*, *FANCF*, *FANCG*, *FANCI*, *FANCJ*, *FANCL*, *FANCM,* and *FANCN* (reviewed in 3). Eight of the proteins (FANCA, FANCB, FANCC, FANCE, FANCF, FANCG, FANCL, FANCM) are thought to assemble into a core nuclear complex, which activates the downstream proteins FANCD2 and FANCI by monoubiquitination (4,5). *FANCD1*, *FANCJ*, and *FANCN* are identical to the breast cancer susceptibility genes *BRCA2*, *BACH1/BRIP1*, and *PALB2*, closely linking the FA and BRCA pathways (3). Presumably, all these gene products participate in a common pathway of repair or processing of interstrand cross-links (ICLs) (2) and DNA double-stranded breaks (DSBs) (6,7) that may arise as intermediates in ICL repair (8).

Analysis of an international database of FA patients has revealed a remarkable predisposition to squamous cell carcinoma (SCC) of the cervix and head and neck (HNSCC) (9,10). The cumulative incidence of SCC in FA patients is 19% by the age of 40 years, with an incidence ratio of 500, making FA the single best genetic model of HNSCC. Human papillomavirus (HPV) may be an initiating factor in FA-HNSCC carcinogenesis, with one group of investigators describing HPV DNA in 84% of FA tumors and absence of *TP53* mutations (11). However, a second study was unable to find HPV in four tumor cell lines established from a different set of FA patients (12). Instead, these FA tumors demonstrated loss of heterozygosity patterns and *TP53*

***Address correspondence and reprint requests to*** *Johnson M. Liu, Les Nelkin Memorial Pediatric Oncology Laboratory, Schneider Children's Hospital, Pediatric Hematology/Oncology & Stem Cell Transplantation, New Hyde Park, NY 11040. Phone: 718-470-7174; Fax: 718-470-4843; E-mail: jliu3@NSHS.edu.*
*Submitted November 26, 2007; accepted for publication January 2, 2008; Epub (www.molmed.org) ahead of print January 22, 2008.*

mutations and polymorphisms similar to the non–FA-associated sporadic HNSCC controls. Although these conflicting results have not been reconciled and the HPV association remains unclear, all available information points to the importance of p53 tumor suppressor mechanisms in the genesis of cancer in FA patients.

The DNA damage response (DDR) is a complex network that regulates cell proliferation and death and coordinates repair in response to DNA damage (13). Checkpoints prevent cells that have sustained DNA damage from transiting the cell cycle before repair, whereas irreparable DNA damage triggers activation of pathways, resulting in removal of affected cells from the replicating pool. The p53 tumor suppressor accumulates in cells treated with ultraviolet or ionizing radiation (IR) and is required for the $G_1$/S cell cycle checkpoint. Similarly, the ataxia telangiectasia mutated (ATM) kinase is stimulated immediately after IR-induced DSB damage (reviewed in 14) and rapidly phosphorylates substrates involved in the DSB response, including p53 and BRCA1. The major control of ATM activity is thought to be by autophosphorylation of preexisting protein (15). Loss of checkpoint function is associated with genomic instability and tumor predisposition, a concept recently validated in studies demonstrating activation of a DDR network early in tumorigenesis (16,17), which may serve as a barrier to cancer progression.

Two recent studies suggested that whereas FA cells could repair IR-generated DSBs, they were deficient in ICL repair (8,18). By contrast, cells deficient in the noncore FANCJ/BACH1/BRIP1 gene product were defective in the resolution of IR-induced DSBs and demonstrated radiosensitivity (19). These findings suggest that there may be differences in the precise roles of the individual FANC gene products, which may contribute to clinical heterogeneity. To clarify the function of the core FA protein, FANCA, we studied the DDR in isogenic pairs of *FANCA*-mutant and gene-corrected primary fibroblast cell lines. Our results suggest a molecular mechanism that may underlie the remarkable cancer predisposition in FA patients.

## MATERIALS AND METHODS

### Cell Lines and Cell Culture

Human primary fibroblasts were obtained from the Coriell Institute (Camden, NJ, USA): GM1309C and GM16631 are *FANCA*-mutant fibroblast lines. These cells were grown in α-modified Eagle's medium containing 15% fetal bovine serum with penicillin/streptomycin. OHSU-974 and VU974L were kindly provided by Dr. Grover Bagby, Oregon Health Sciences University. OHSU-974 was grown in 1:1 DMEM/F12 medium containing 1 μM hydrocortisone, 10 μg/mL bovine insulin, 10% fetal bovine serum, and penicillin and streptomycin. VU974L was grown in RPMI containing 2 mM L-glutamine, 15% fetal bovine serum, and penicillin/streptomycin.

### Retroviral Transduction

Retroviral vectors expressing human FANCA were produced in Phoenix packaging cells with amphotropic envelope (originally from Dr. G.P. Nolan, Stanford University) by transfecting pBabe-Puro-FANCA. GM1309C and GM16631 cells were infected with retroviral vectors and selected in medium containing puromycin 1 μg/mL or blasticidin S 2 μg/mL. Cells were checked for MMC sensitivity by the crystal violet assay and cell cycle analyses to confirm phenotypic correction following transduction of wild-type FANCA.

### Immunoblot Analysis

Cells were harvested 2 h after irradiation (Cs-137; Gammacell 1000, AECL, Ottawa, Canada) or 24 h after MMC treatment (0.1 or 1 μM). Cell extracts were prepared in EBC buffer (50 mM Tris, pH 8, 120 mM NaCl, 0.5% Nonidet P-40) with the addition of 2 μg/mL aprotinin, 2 μg/mL leupeptin, and 100 μg/mL polymethylsulfonyl fluoride. Protein concentration was determined using the BCA Protein Assay (Pierce Biotechnology, Rockford, IL, USA), and 50 μg whole cell extract was loaded per lane and subjected to 6%, 7.5%, 10%, or 15% SDS-PAGE. Transfer to PVDF was performed using a semidry transfer method (Trans-Blot; Bio-Rad, Hercules, CA, USA). After blocking with 1% nonfat dried milk in phosphate-buffered saline/0.1% Tween 20, the primary antibody was added in 1% nonfat dried milk in phosphate-buffered saline/0.1% Tween 20 overnight. The secondary antibodies used were peroxidase-conjugated goat antimouse IgG, goat antirabbit IgG (Santa Cruz Biotechnology, Santa Cruz, CA, USA), or swine antigoat IgG (Roche) at 1:5000 in 1% nonfat dried milk in phosphate-buffered saline/0.1% Tween 20. Signals were visualized using the ECL kit (Pierce Biotechnology).

Antibodies used in these studies were against ATM (GeneTex, San Antonio, TX, USA); ATMSer1981 (Rockland, Gilberts ville, PA, USA); CHK2, p53, p21, FANCA, and β-actin (Santa Cruz Biotechnology); CHK2Thr68, p53Ser15, and tubulin (Cell Signaling, Danvers, MA, USA); and PP2A(C) (BD Transduction Laboratories, Franklin Lakes, NJ, USA).

### Transient and Stable Knockdown of FANCA and Q-PCR

Four HuSH 29-mer short-hairpin RNA (shRNA) constructs were generated against human *FANCA* (OriGene Technologies, Rockville, MD, USA). Every shRNA construct was cloned in the pRS plasmid vector under the control of the U6 promoter. The following shRNA sequences were used: 1, TGCTGTCGTC ACATCTGACCTCAAATAGC; 2, AGCCA GCGTGATGTTATATCGGCACAGGT; 3, CTGCCTTTGTGAACAGATGGAAGCA TCCT; and 4, AGATGCGAGCAGTTC TTCCACTTGGTCAA.

Control vectors expressed either shRNA against GFP or no shRNA. The different constructs were transfected into HCT116 cells using Fugene reagent (Roche). For transient studies, cells were harvested 48 h after transfection, and

RNA was analyzed by quantitative PCR (Q-PCR). For studies with stable clones, transfected cells were cultured under puromycin (Sigma) selection at 2 μg/mL. Total RNA from either transient or stable clones was extracted with Trizol reagent (Invitrogen, Carlsbad, CA, USA) and analyzed for FANCA and ATM expression by Q-PCR.

Q-PCR was performed on the 7900HT Fast Real-Time PCR System (Applied Biosystems, Foster City, CA, USA) to measure the levels of *FANCA* (NM_000135.2) or *ATM* (NM_000051) using TaqMan and Universal Probe Library technology and *CYPB* as a control.

### Immunofluorescence and Confocal Microscopy

Primary fibroblasts were grown on chamber slides (Nunc). After the indicated cultivation times following 5 or 0.5 Gy irradiation, cells were fixed with 4% paraformaldehyde for 10 min. For MMC treatment, cells were incubated with 3 μM MMC for 1 h. After two washes with PBS, cells were cultivated for the indicated times and fixed. After fixation, cells were permeabilized for 10 min in 0.3% Triton-X/PBS, washed twice with PBS, and blocked with 3% bovine serum albumin/PBS for 30 min. The cells were then incubated with rabbit or mouse anti–γ-H2AX phospho-Ser139 (Upstate, Charlottesville, VA, USA) for 1 h at room temperature, washed three times in PBS, and incubated with Alexa Fluor 488 or Alexa Fluor 594 conjugated antirabbit or antimouse IgG (Molecular Probes). Cells were washed three times in PBS and mounted by using Slowfade Antifade solution (Molecular Probes-Invitrogen, Eugene, OR, USA). Fluorescence images were captured using an Olympus IX70 confocal microscope. γ-H2AX foci were enumerated manually after capturing images, and cells containing more than five discrete bright dots were scored positive. More than 150 morphologically intact cells were examined for each experiment and time point. Standard error of the mean (SEM) was calculated.

### Flow Cytometric Assessment of Cell Cycle Arrest and Apoptosis

FA cell lines were exposed to varying concentrations of nitrogen mustard (NM) and studied for onset of cell cycle arrest and apoptosis using flow cytometry. Apoptotic cells were identified by fluorescent end labeling of DNA fragments using terminal deoxynucleotidyl transferase nick-end labeling (TUNEL), with a DAPI or propidium iodide DNA counterstain. $G_2$/M arrest was assessed by ploidy analysis after DNA staining with propidium iodide.

### *TP53* Mutation Testing

Genomic DNA was isolated from cells using a kit from Gentra Systems (Minneapolis, MN, USA). Mutation detection for the *TP53* gene was done using a commercial chip and resequencing (Asper Biotech, Tartu, Estonia).

## RESULTS

### Upregulated ATM Gene Expression and Activation of the ATM-p53-Checkpoint Pathway in Primary Fibroblasts Derived from FA Patients

To study the functional relationship between the p53-ATM axis and the FA gene pathway, we used the following patient-derived primary fibroblast cell lines: *FANCA*-mutant GM1309C and GM16631 and corresponding gene-corrected cell lines created by transduction with wild-type FANCA cDNA. For each transduced line, complementation of the FA phenotype was confirmed by correction of MMC sensitivity and relief of $G_2$/M cell cycle delay at 48 h after treatment with MMC (data not shown). We first analyzed the expression levels of components of the p53-ATM axis and also activation of this pathway using antiphosphoprotein antibodies. In GM1309C cells, basal expression of ATM and p53 and phosphorylation of ATM (Ser1981) and p53 (Ser15) induced by IR or MMC were upregulated, compared with GM1309C cells transduced with wild-type FANCA (Figure 1A). Similar results were observed in a second *FANCA*-mutant line, GM16631 (Figure 1B). We reasoned that these results might be explained by upregulation of the basal levels of ATM protein in the mutant fibroblasts. We also confirmed the upregulation of ATM protein (Figure 1C) in a *FANCA*-mutant EBV-immortalized lymphoblastoid cell line, HSC72, in comparison to its gene-corrected control. Using real-time Q-PCR assays, we confirmed that *ATM* gene expression was increased in GM1309C cells (Q-PCR fold change: GM1309c mutant 1.00 vs. gene-corrected control 0.45) and in HSC72 cells (Q-PCR fold change: HSC72 mutant 0.42 vs. gene-corrected control 0.19).

To determine if these changes in *ATM* gene expression were directly caused by FANCA depletion, we transfected HCT116 cells (known to be p53 wild-type) with two different siRNAs against *FANCA*. For these experiments, we used a plasmid expression vector (pRS; OriGene Technologies) that drives 29-mer short hairpin RNAs targeting *FANCA*. In both transient and stable transfection experiments with either shRNA (Table 1), we found that knockdown of *FANCA* expression was associated with moderate downregulation of *ATM* expression, as assessed by real-time PCR, compared with cells transfected with an empty vector control. These data suggested that depletion of FANCA does not directly lead to upregulated *ATM* gene expression.

### γ-H2AX Foci in Primary *FANCA*-Mutant Fibroblasts

γ-H2AX foci are regarded as sensitive markers of DSB formation (20). Thus, we next asked whether FA mutant cells accumulate larger numbers of DSBs, because FA cells are presumed to be defective in the processing or repair of DSBs that arise during ICL repair (2). Using semiquantitative immunofluorescent microscopy, we analyzed γ-H2AX focus formation in the primary *FANCA*-mutant GM1309C cell line and its gene-corrected control after exposure to IR or MMC. (For both cell lines, it was possible to detect baseline γ-H2AX staining of approximately 3% to 7% of cells, with no

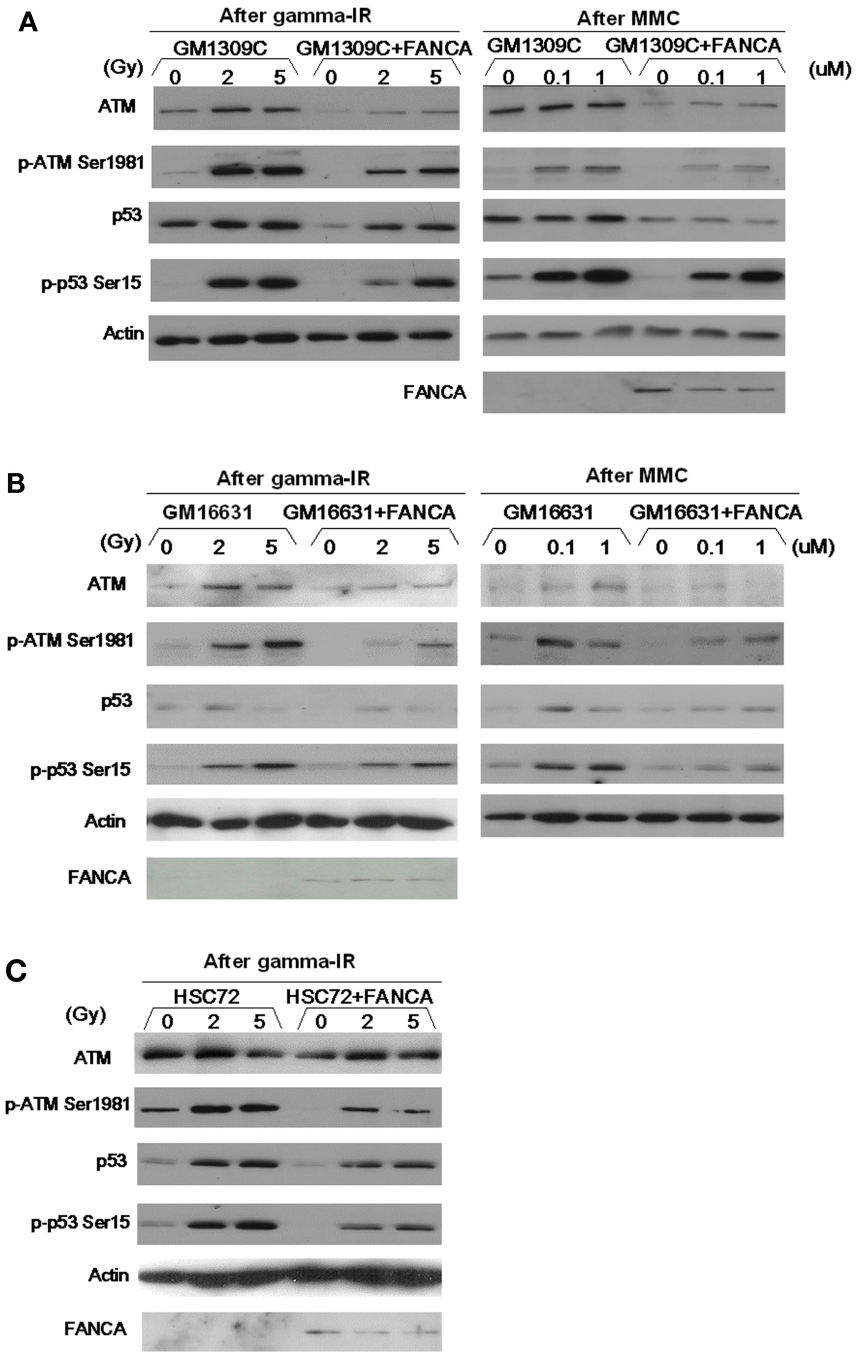


**Figure 1.** Heightened activation of ATM-p53 axis in *FANCA*-mutant cells compared with gene-complemented cells. In *FANCA*-mutant primary fibroblast cells, basal expression of ATM and p53 and phosphorylation of ATM (Ser1981) and p53 (Ser15) induced by IR or MMC were upregulated, compared with identically treated isogenic mutant cells transduced with wild-type FANCA. (A) GM1309C and isogenic control cells transduced with wild-type FANCA; (B) GM16631 and isogenic control cells transduced with wild-type FANCA. Left columns: cells were harvested and lysed 2 hrs after γ irradiation at indicated doses. Right columns: Cells were harvested and lysed 24 h after MMC treatment at indicated doses. (C) HSC72 and isogenic control cells transduced with wild-type FANCA. Postirradiation samples are shown.

significant difference between the two.) γ-H2AX foci could easily be seen after IR (Figure 2A) or MMC (Figure 2B) treatment, but the kinetics and time course of formation were markedly different with each type of DNA damage (Figure 3A and B). Following IR exposure, γ-H2AX foci were rapidly formed (within minutes) in FA-mutant and gene-corrected cells (Figure 2A). Comparing the FA mutant and gene-corrected cell lines, however, there was no significant difference in the numbers of cells positive for γ-H2AX foci, and there was rapid clearance of γ-H2AX foci in both mutant and control cells (Figure 3A). Even after lowering the IR dose from 5 to 0.5 Gy, there was no difference in the percentage of foci-positive cells between GM1309C and its gene-corrected control (data not shown). With the lower 0.5 Gy dose, the mean number of foci per cell decreased as expected, but there was no significant difference in the means between GM1309C and control cells (data not shown).

For MMC, a concentration of 3 μM was chosen because this had previously been shown to induce γ-H2AX foci in primary MEF cells (21) and is thought to induce approximately $10^3$ interstrand crosslinks per genome. After MMC treatment (Figure 2B and Figure 3B), the number of cells exhibiting γ-H2AX foci increased gradually over 24 to 48 h, and the peak of positively scored cells (~60%) was less than following IR (90%–100%). In contrast to the results following IR, we observed a significant increment and persistence in the number of cells positive for γ-H2AX foci in *FANCA*-mutant primary fibroblasts compared with gene-corrected controls.

### Acquired Relative Resistance to DNA Crosslinker-Induced Cell Cycle Arrest and Apoptosis in a *TP53*-Mutant, Patient-Derived HNSCC Cell Line

To this point, our experiments had focused on primary fibroblast cell lines derived from FA patients. To determine the significance of our findings with respect to FA carcinogenesis, we next turned to a

**Table 1.** Depletion of FANCA by RNA interference does not directly lead to increased *ATM* gene expression as assessed by Q-PCR.

| | Transient | | | Stable | | |
|---|---|---|---|---|---|---|
| | siRNA 1 | siRNA 3 | Control | siRNA 1 | siRNA 3 | Control |
| H-CYPB | | | | | | |
| Average | 21.11 | 21.31 | 20.91 | 20.87 | 20.53 | 19.52 |
| SD | 0.03 | 0.00 | 0.01 | 0.00 | 0.05 | 0.17 |
| H-FANCA | | | | | | |
| Average | 27.11 | 27.60 | 25.86 | 26.96 | 26.80 | 24.61 |
| SD | 0.00 | 0.19 | 0.02 | 0.15 | 0.02 | 0.17 |
| Delta Ct | 6.00 | 6.29 | 4.95 | 6.09 | 6.27 | 5.09 |
| SD | 0.03 | 0.19 | 0.02 | 0.15 | 0.06 | 0.24 |
| Test-control | 1.05 | 1.34 | 0.00 | 1.00 | 1.18 | 0.00 |
| Fold change | 0.48 | 0.40 | 1.00 | 0.50 | 0.44 | 1.00 |
| H-ATM | | | | | | |
| Average | 25.89 | 26.71 | 25.04 | 24.83 | 24.96 | 22.87 |
| SD | 0.05 | 0.00 | 0.00 | 0.15 | 0.08 | 0.14 |
| Delta Ct | 4.78 | 5.40 | 4.13 | 3.95 | 4.44 | 3.36 |
| SD | 0.06 | 0.01 | 0.01 | 0.15 | 0.10 | 0.22 |
| Test-control | 0.65 | 1.27 | 0.00 | 0.59 | 1.08 | 0.00 |
| Fold change | 0.64 | 0.41 | 1.00 | 0.66 | 0.47 | 1.00 |

Either transient (left columns) or stable (right columns) transfection of shRNA against *FANCA* was performed: *FANCA* shRNA sequences 1, 3, and empty vector control, respectively. Knockdown of FANCA mRNA expression by either shRNA construct was confirmed when compared with the empty vector control (assigned a value of 1.0). Transient or stable depletion of FANCA mRNA expression led to modestly decreased levels of *ATM* gene expression. All comparisons were made using human cyclophilin B (H-CYPB) as an internal control. Shown are: Average cycle threshold; SD; delta Ct (difference between Ct of test and the H-CYPB internal control); test – control (difference between delta Ct of test and the empty vector control); fold change ($1/2^{\Delta-\Delta Ct}$).

patient-derived HNSCC cell line. The HPV-negative squamous cell carcinoma cell line OHSU-974 (12) is derived from a FA-A patient, and VU974L is a lymphoblastoid cell line derived from this same individual. Both cell lines were exposed to varying concentrations of the DNA cross-linker NM and studied for onset of cell cycle arrest and apoptosis as described in "Materials and Methods." At each NM concentration, the percentage of cells arrested in $G_2$/M and the percentage of apoptotic cells were quantified. Threshold NM concentrations for increased G2/M arrest and apoptosis were then correlated. Accumulation of apoptotic cells did not occur until these thresholds were met or exceeded. Figure 4A displays the percentage of cells arrested in $G_2$/M as a function of NM concentration for the respective cell lines. VU974L retained heightened sensitivity to NM, whereas OHSU-974 exhibited resistance to NM-induced cell cycle arrest. As shown in Figure 4B, VU974L underwent NM-induced apoptosis with concentrations of NM that exceeded the threshold for G2/M arrest. In contrast, OHSU-974 displayed a marked resistance to NM-induced apoptosis at the concentrations of NM tested. In considering these results, it is important to recognize that the resistance to cell cycle arrest and apoptosis is only relative to VU974L, because OHSU-974 is more sensitive to DNA crosslinker cytotoxicity than are HNSCC cell lines derived from non-FA patients (12).

OHSU-974 was previously described as having a 1-bp deletion at codon 41 (exon 4) of *TP53*, which results in a very short p53 protein by introduction of a stop codon downstream of this frameshift mutation (12). In addition, OHSU-974 was also determined to have a polymorphism encoding arginine or proline at position 72 of p53 (12). When we analyzed the *TP53* gene from genomic DNA of VU974L, we confirmed the presence of the heterozygous polymorphism at exon 4 (codon 72) but found no other *TP53* mutations among 1319 mutations or SNPs tested (data not shown).

## DISCUSSION

We focused our experiments on the DDR in primary FA cells and its putative role as a barrier to cancer through cell cycle and apoptosis regulation. In FA mutant cells, we found increased IR- or MMC-induced phosphorylation of p53 and ATM, suggesting a generally heightened activation responding to DNA damage. This heightened response could be explained by upregulation of *ATM* gene expression in the *FANCA*-mutant cell lines. Functional analysis of this response using γ-H2AX foci as sensitive markers of DSBs suggested that FA-A fibroblasts suffer from a defect that causes aberrant persistence of MMC-induced foci. The consequences of this chronically activated DDR may include selective pressure for cancer cells that can escape this checkpoint barrier.

Our immunoblot analysis suggests increased basal levels of ATM in the FA mutant fibroblast cell lines compared with that of gene-corrected controls, thereby explaining heightened activation of ATM and p53 following either IR or MMC treatment. There may also be slight upregulation of phosphorylated ATM even before IR or MMC, suggesting a response to endogenous DNA damage. In human fibroblasts, ATM levels are thought to remain relatively constant throughout the cell cycle (22), and it is well established that the major control of ATM function is by activation of preexisting protein by a mechanism involving autophosphorylation (15). However, recent experiments indicate that ATM expression can also be regulated at the transcriptional level (23). The E2F-1 transcription factor increases ATM promoter

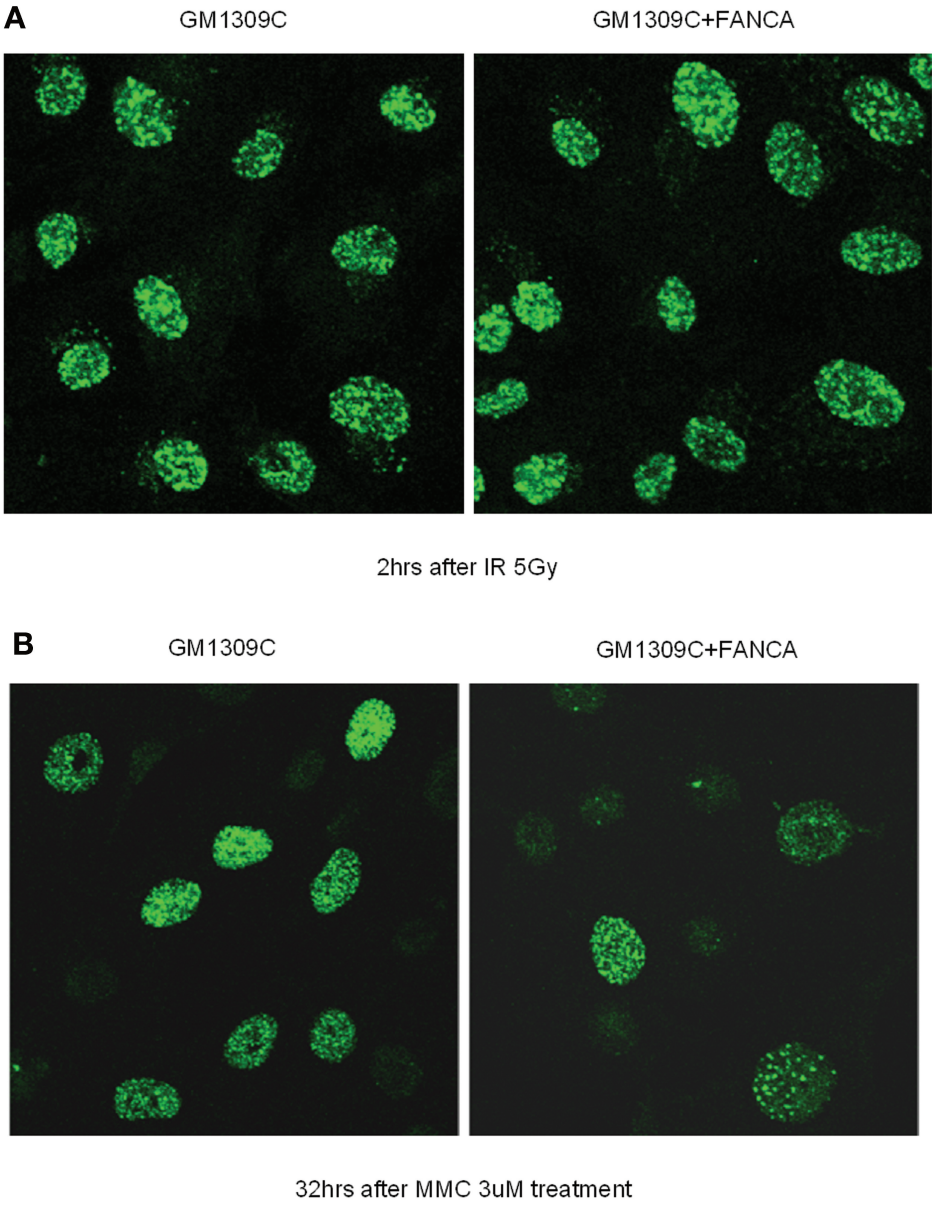


**Figure 2.** IR-induced and MMC-induced γ-H2AX foci in *FANCA*-mutant primary fibroblast cells compared with gene-corrected controls. (A) After 5 Gy irradiation, GM1309C and gene-corrected control cells were incubated for 2 h at 37°C and stained with anti–γ-H2AX. (B) After 1-h incubation with 3 μM MMC, GM1309C and gene-corrected control cells were washed to remove MMC, further incubated for 48 h at 37°C, and stained with anti–γ-H2AX.

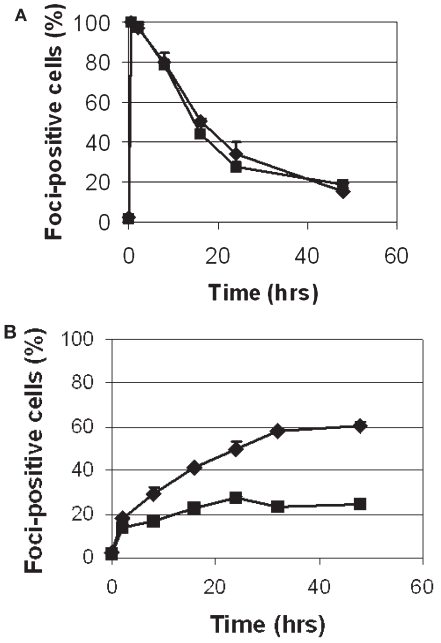


**Figure 3.** Kinetics of IR-induced and MMC-induced γ-H2AX foci in *FANCA*-mutant primary fibroblast cells compared with gene-corrected controls. (A) Kinetics and time course of cells scored positive for γ-H2AX foci up to 48 h after irradiation. (B) Kinetics and time course of cells scored positive for γ-H2AX foci up to 48 h after MMC washout. Diamond, GM1309C; square, gene-corrected control. Error bars represent SEM.

activity (24), and a deficiency in the catalytic subunit of DNA-dependent protein kinase leads to downregulation of ATM (25). To our knowledge, however, increased ATM gene expression in *FANCA*-mutant cells has not been previously described and represents a potentially important mechanism. Our data also indicate that knockdown of *FANCA* does not directly lead to upregulation of ATM expression, perhaps because chronic genotoxic stress induced by loss of FANCA is not seen in cells partially depleted of FANCA.

A second important question is, why should ATM be hyperactivated after IR when our γ-H2AX data indicate that FA cells are proficient at DSB repair, the main lesion induced by IR? IR-induced ATM activation in FA cells may result from damage to biomolecules including lipids and DNA (single-strand breaks, DSBs, and nucleotide damage), as well as the formation of reactive oxygen species (ROS) (26). Previously, we demonstrated a possible role for FA proteins in protection against oxidative DNA damage (27). Viewed in this context, ATM activation may reflect a response to increased levels of endogenous and induced oxidative DNA damage that includes but is not necessarily limited to DSBs.

Phosphorylated γ-H2AX accumulates at DSBs, forming foci that can be de-

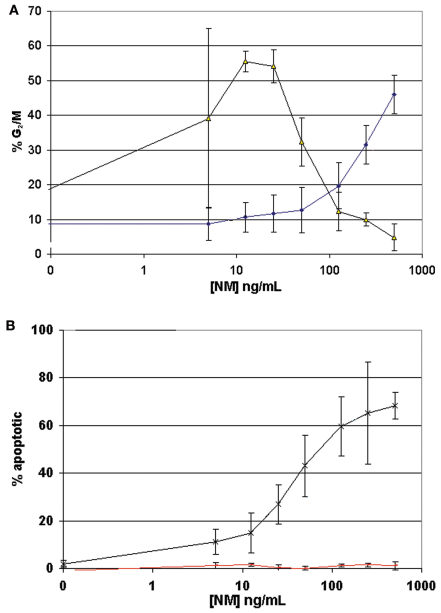


**Figure 4.** Relative resistance to DNA crosslinker-induced cell cycle arrest and apoptosis in a *TP53*-mutant, patient-derived HNSCC cell line. (A) Percentage of cells arrested in $G_2$/M as a function of NM concentration for VU974L (black) and OHSU-974 (blue). VU974L retained heightened sensitivity to NM-induced cell cycle arrest, reaching a threshold and then decreasing. By comparison, OHSU-974 exhibited a relative resistance to NM-induced cell cycle arrest. (B) Percentage of apoptotic cells as a function of NM concentration for VU974L (black) and OHSU-974 (red). VU974L underwent NM-induced apoptosis with concentrations of NM that exceeded the threshold for $G_2$/M arrest. By contrast, OHSU-974 displayed a marked resistance to NM-induced apoptosis at the concentrations of NM tested.

tected by immunostaining (20). Using confocal microscopy to enumerate γ-H2AX foci, our data indicate marked differences in the formation and persistence of DSBs in FA mutant cells only following MMC treatment. If we consider our data in the context of a recently proposed model of the FANC proteins in DNA ICL repair (2), which proposes DSB intermediates, several conclusions can be drawn. First, our data suggest that the processing and clearance of IR-induced DSBs are not grossly impaired in FA mutant primary cells. Following IR, there was a very rapid formation followed by a rapid clearance of DSBs, with no differences between FA mutant and control cells. Following MMC, however, DSBs were gradually increased until reaching a plateau, with markedly higher levels in FA mutant cells before a correspondingly higher plateau phase. Our findings are similar to those reported by Rothfuss and Grompe (8) and Atanassov et al. (18), although neither study employed isogenic pairs of patient-derived primary fibroblasts as we have done. In particular, the study by Rothfuss and Grompe (8) demonstrated in normal cells rapid activation of (ubiquitinated) FANCD2 after IR and slow activation in S phase after ICL treatment, data that closely mirror our γ-H2AX foci results. ICLs are believed to be repaired predominantly by homologous recombination (HR) pathways, whereas DSBs are repaired by both HR and nonhomologous end joining (NHEJ) processes (for review see 28). Thus, persistence of γ-H2AX foci in FA cells following MMC may reflect inefficient HR, while clearance of IR-induced DSBs may indicate intact NHEJ (18).

FANCJ was identified as the BRIP1 (BRCA1-interacting protein 1) or BACH1 (BRCA1-associated C-terminal helicase 1) helicase (29,30). In recently published work, MCF-7 breast cancer cells made deficient for BACH1 by RNA interference methods were delayed in DNA double-strand break repair, exhibiting persistence of γ-H2AX foci following 0.5 Gy IR treatment (19). Although these experiments differ from ours in that shRNA methods were used to knock down BACH1 expression, they suggest that FANCJ deficiency has different effects on DSB repair and IR sensitivity than do mutations in *FANCA*. In this regard, FANCJ is known to act downstream from the core complex FA pathway, as ubiquitination of FANCD2 is normal in FA-J cells (31). Possibly, these differences in DSB processing between FANCJ and FANCA may have clinical significance.

Turning to the implications of our work for carcinogenesis, mutant FA primary fibroblasts are known to be 3- to 50-fold more sensitive than normal fibroblasts to transformation in culture by the SV40 virus (32). In previous work, we confirmed this marked susceptibility to transformation of a FA-C mutant primary fibroblast cell line, GM449 (33). We then introduced a copy of the wild-type FANCC cDNA into GM449 cells using a recombinant adeno-associated virus (rAAV) vector. We found that GM449 cells transduced with FANCC were at least 10-fold less prone to form transformed foci. Diminished transformation potential of transduced cells was a specific effect of FANCC because GM449 cells transduced with a rAAV vector not containing FANCC retained marked susceptibility to SV40 transformation. At the time of these studies, we speculated that FA gene products such as FANCC might have a tumor suppressor function cooperative with p53 or RB. Recent genetic evidence for this comes from the demonstration of accelerated tumor formation in both *Fancc* (34) and *Fancd2* (35) knockout mice bred to heterozygosity at *Trp53*. Paradoxically, our present data, which indicate DDR activation in mutant cells, suggest intact or even hyperactive tumor suppressor pathways in mutant cells responding to MMC-induced damage. In zebrafish, knockdown of Fancd2 caused developmental abnormalities that were attributed to p53-dependent apoptosis (36). Consequently, we hypothesize that chronic DDR activation, perhaps resulting from defective DNA processing and repair, may drive antiproliferative signaling at various points during development and lead to somatic abnormalities and bone marrow failure. Conversely, this same state may exert significant selective pressure for the inactivation of p53 or other DDR components, accelerating genetic instability and evolution of leukemia and cancer.

A recent publication has suggested that *FANCG*- and *FANCC*-deficient pancreatic tumor cell lines are hypersensitive to inhibition of ATM by the KU-55933 in-

hibitor (37). The two cell lines, Hs766T and PL11, are not derived from FA patients but have mutation of one allele and loss of heterozygosity of the other allele of *FANCG* or *FANCC*, respectively (38). Both cell lines were previously shown to be hypersensitive to DNA crosslinkers as assessed by cell survival assays and $G_2$/M cell cycle arrest (39). By comparison, our data from OHSU-974, an HNSCC cell line established from a known patient with biallelic mutations in *FANCA*, indicate loss of DNA crosslinker-induced checkpoint control, the mechanism of which is currently the focus of our ongoing research. Although based on this single cell line, our observations suggest that a subset of FA patient-derived HNSCC may acquire secondary mutations that enable escape from dependence on the ATM surveillance pathway.

## ACKNOWLEDGMENTS

We gratefully acknowledge grant support for J.M. Liu (The Nelkin Foundation and Fanconi Anemia Research Fund, Inc.) and T. Ouchi (CA79892 and CA90631).

## REFERENCES

1. Liu JM, Dokal I (2006) Constitutional aplastic anemias. In *Clinical Hematology* (Young NS, Gerson SL, High KA, eds.), Elsevier.
2. Niedernhofer LJ, Lalai AS, Hoeijmakers JH (2005) Fanconi anemia (cross)linked to DNA repair. *Cell* 123:1191–8.
3. Wang W (2007) Emergence of a DNA-damage response network consisting of Fanconi anaemia and BRCA proteins. *Nat. Rev. Genet.* 8:735–48.
4. Garcia-Higuera I, Taniguchi T, Ganesan S, Meyn MS, Timmers C, Hejna J, Grompe M, D'Andrea AD (2001) Interaction of the Fanconi anemia proteins and BRCA1 in a common pathway. *Mol. Cell* 7:249–62.
5. Sims AE, et al. (2007) FANCI is a second monoubiquitinated member of the Fanconi anemia pathway. *Nat. Struct. Mol. Biol.* 14:564–7.
6. Stewart G, Elledge SJ (2002) The two faces of BRCA2, a FANCtastic discovery. *Mol. Cell* 10:2–4.
7. D'Andrea AD, Grompe M (2003) The Fanconi anaemia/BRCA pathway. *Nat. Rev. Cancer* 3:23–34.
8. Rothfuss A, Grompe M (2004) Repair kinetics of genomic interstrand DNA cross-links: evidence for DNA double-strand break-dependent activation of the Fanconi anemia/BRCA pathway. *Mol. Cell Biol.* 24:123–34.
9. Rosenberg PS, Greene MH, Alter BP (2003) Cancer incidence in persons with Fanconi anemia. *Blood* 101:822–6.
10. Kutler DI, et al. (2003) High incidence of head and neck squamous cell carcinoma in patients with Fanconi anemia. *Arch. Otolaryngol. Head Neck Surg.* 129:106–12.
11. Kutler DI, et al. (2003) Human papillomavirus DNA and p53 polymorphisms in squamous cell carcinomas from Fanconi anemia patients. *J. Natl. Cancer Inst.* 95:1718–21.
12. van Zeeburg HJ, et al. (2005) Generation and molecular characterization of head and neck squamous cell lines of Fanconi anemia patients. *Cancer Res.* 65:1271–6.
13. Zhou BB, Elledge SJ (2000) The DNA damage response: putting checkpoints in perspective. *Nature* 408:433–9.
14. Kastan MB, Lim DS (2000) The many substrates and functions of ATM. *Nat. Rev. Mol. Cell Biol.* 1:179–86.
15. Bakkenist CJ, Kastan MB (2003) DNA damage activates ATM through intermolecular autophosphorylation and dimer dissociation. *Nature* 421:499–506.
16. Bartkova J, et al. (2005) DNA damage response as a candidate anti-cancer barrier in early human tumorigenesis. *Nature* 434:864–70.
17. Gorgoulis VG, et al. (2005) Activation of the DNA damage checkpoint and genomic instability in human precancerous lesions. *Nature* 434:907–13.
18. Atanassov BS, Barrett JC, Davis BJ (2005) Homozygous germ line mutation in exon 27 of murine Brca2 disrupts the Fancd2-Brca2 pathway in the homologous recombination-mediated DNA interstrand cross-links' repair but does not affect meiosis. *Genes Chromosomes Cancer* 44:429–37.
19. Peng M, Litman R, Jin Z, Fong G, Cantor SB (2006) BACH1 is a DNA repair protein supporting BRCA1 damage response. *Oncogene* 25:2245–53.
20. Rogakou EP, Pilch DR, Orr AH, Ivanova VS, Bonner WM (1998) DNA double-stranded breaks induce histone H2AX phosphorylation on serine 139. *J. Biol. Chem.* 273:5858–68.
21. Niedernhofer LJ, et al. (2004) The structure-specific endonuclease Ercc1-Xpf is required to resolve DNA interstrand cross-link-induced double-strand breaks. *Mol. Cell Biol.* 24:5776–87.
22. Brown KD, et al. (1997) The ataxia-telangiectasia gene product, a constitutively expressed nuclear protein that is not up-regulated following genome damage. *Proc. Natl. Acad. Sci. U. S. A.* 94:1840–5.
23. Gueven N, Fukao T, Luff J, Paterson C, Kay G, Kondo N, Lavin MF (2006) Regulation of the Atm promoter in vivo. *Genes Chromosomes Cancer* 45:61–71.
24. Berkovich E, Ginsberg D (2003) ATM is a target for positive regulation by E2F-1. *Oncogene* 22:161–7.
25. Peng Y, et al. (2005) Deficiency in the catalytic subunit of DNA-dependent protein kinase causes down-regulation of ATM. *Cancer Res.* 65:1670–7.
26. Kurz EU, Lees-Miller SP (2004) DNA damage-induced activation of ATM and ATM-dependent signaling pathways. *DNA Repair (Amst)* 3:889–900.
27. Futaki M, et al. (2002) The FANCG Fanconi anemia protein interacts with CYP2E1: possible role in protection against oxidative DNA damage. *Carcinogenesis* 23:67–72.
28. Futaki M, Liu JM (2001) Chromosomal breakage syndromes and the BRCA1 genome surveillance complex. *Trends Mol. Med.* 7:560–5.
29. Levitus M, et al. (2005) The DNA helicase BRIP1 is defective in Fanconi anemia complementation group J. *Nat. Genet.* 37:934–5.
30. Levran O, et al. (2005) The BRCA1-interacting helicase BRIP1 is deficient in Fanconi anemia. *Nat. Genet.* 37:931–3.
31. Bridge WL, Vandenberg CJ, Franklin RJ, Hiom K (2005) The BRIP1 helicase functions independently of BRCA1 in the Fanconi anemia pathway for DNA crosslink repair. *Nat. Genet.* 37:953–7.
32. Todaro GJ, Green H, Swift MR (1966) Susceptibility of human diploid fibroblast strains to transformation by SV40 virus. *Science* 153:1252–4.
33. Liu JM, Poiley J, Devetten M, Kajigaya S, Walsh CE (1996) The Fanconi anemia complementation group C gene (FAC) suppresses transformation of mutant fibroblasts by the SV40 virus. *Biochem. Biophys. Res. Commun.* 223:685–90.
34. Freie B, et al. (2003) Fanconi anemia type C and p53 cooperate in apoptosis and tumorigenesis. *Blood* 102:4146–52.
35. Houghtaling S, et al. (2005) Heterozygosity for p53 ($Trp53^{+/-}$) accelerates epithelial tumor formation in Fanconi anemia complementation group D2 (Fancd2) knockout mice. *Cancer Res.* 65:85–91.
36. Liu TX, et al. (2003) Knockdown of zebrafish Fancd2 causes developmental abnormalities via p53-dependent apoptosis. *Dev. Cell* 5:903–14.
37. Kennedy RD, et al. (2007) Fanconi anemia pathway-deficient tumor cells are hypersensitive to inhibition of ataxia telangiectasia mutated. *J. Clin. Invest* 117:1440–9.
38. van der Heijden MS, Yeo CJ, Hruban RH, Kern SE (2003) Fanconi anemia gene mutations in young-onset pancreatic cancer. *Cancer Res.* 63:2585–8.
39. van der Heijden MS, et al. (2004) Functional defects in the Fanconi anemia pathway in pancreatic cancer cells. *Am. J. Pathol.* 165:651–7.